BIOCHEMISTRY

 Volume 46, Number 9 March 6, 2007

Current Topics

Respiratory Complex I: Mechanistic and Structural Insights Provided by the Crystal Structure of the Hydrophilic Domain†

Leonid A. Sazanov*

Medical Research Council Dunn Human Nutrition Unit, Wellcome Trust/MRC Building, Hills Road, Cambridge CB2 2XY, U.K.

Received December 5, 2006; Revised Manuscript Received January 18, 2007

ABSTRACT: Complex I of respiratory chains plays a central role in cellular energy production. Mutations in its subunits lead to many human neurodegenerative diseases. Recently, a first atomic structure of the hydrophilic domain of complex I from *Thermus thermophilus* was determined. This domain represents a catalytic core of the enzyme. It consists of eight different subunits, contains all the redox centers, and comprises more than half of the entire complex. In this review, novel mechanistic implications of the structure are discussed, and the effects of many known mutations of complex I subunits are interpreted in a structural context.

Complex I (NADH:ubiquinone oxidoreductase, EC 1.6.5.3) is the first enzyme of the mitochondrial and bacterial respiratory chains. It catalyzes the transfer of two electrons from NADH to quinone, coupled to the translocation of approximately four protons across the membrane, contributing to the proton-motive force required for the synthesis of ATP (*1*, *2*). The mitochondrial enzyme consists of 45 different subunits (*3*, *4*) and is one of the largest known membrane protein complexes, of ~980 kDa. The prokaryotic enzyme is simpler and consists of 13−15 subunits with a combined molecular mass of ~550 kDa (*2*, *5*). Analogues of all conserved subunits of bacterial complex I are found in the mitochondrial enzyme (*1*), and they contain equivalent redox components (*2*). Both mitochondrial and bacterial enzymes have a characteristic L-shaped structure, with the hydrophobic arm embedded in the membrane and the hydrophilic peripheral arm protruding into the mitochondrial matrix or the bacterial cytoplasm (*6*−*9*). Thus, the bacterial enzyme represents a "minimal" model of complex I. Because of its central role in respiration, mutations in subunits of complex I can lead to many human neurodegenerative diseases (*10*). Also, complex I has been suggested to be a major source of reactive oxygen species (ROS) in mitochondria, which can damage mtDNA and may be one of the causes of aging (*11*). Parkinson's disease, at least in its sporadic form, may be caused by an increased level of ROS production from malfunctioning complex I (*12*).

The hydrophilic domain (peripheral arm) of complex I contains the NADH binding site, the primary electron acceptor flavin mononucleotide (FMN),[1] and eight or nine iron−sulfur (Fe−S) clusters (*2*, *13*, *14*), comprising the catalytic core of the enzyme. The proton-pumping machinery must reside in the membrane arm. Recently, we have determined the first atomic structure of the hydrophilic domain of complex I, using the enzyme from *Thermus thermophilus* (*14*, *15*). In this review, I will discuss the features and implications of the structure which were beyond the scope of these initial publications.

† This work was funded by the Medical Research Council.

* To whom correspondence should be addressed. E-mail: sazanov@mrc-dunn.cam.ac.uk. Phone: +44-1223-252910. Fax: +44-1223-252915.

[1] Abbreviations: E_m, midpoint redox potential; FMN, flavin mononucleotide; UQ, ubiquinone; MQ, menaquinone.

10.1021/bi602508x CCC: $37.00
Published on Web 02/03/2007

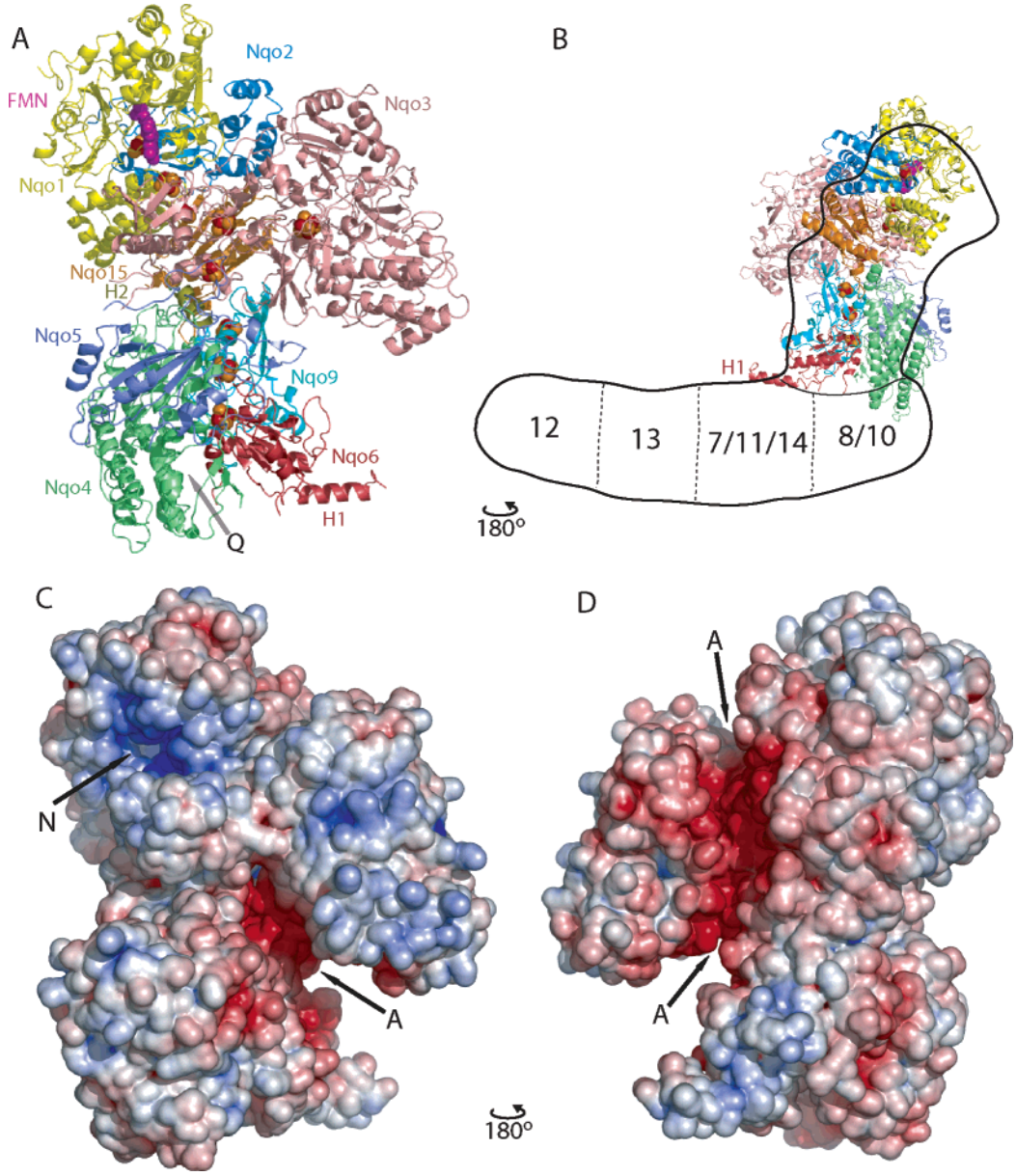

FIGURE 1: Overview of PDB entry 2FUG. (A) Side view, with the membrane arm likely to be beneath and extending to the right, in the direction of helix H1. Each subunit is colored differently. FMN is shown as magenta spheres; Fe atoms are shown as red spheres and S atoms as yellow spheres. Helix H2 is colored olive. (B) A view rotated by 180°, showing a model of a likely mode of attachment of the peripheral domain to the membrane domain. The outline of intact *E. coli* complex I comes from single-particle analysis (*9*), and the model of subunit arrangement is derived from fragmentation studies (*49*). Numbers indicate hydrophobic Nqo subunits. The fit is partially based on the cryo-EM three-dimensional model of *E. coli* complex I (D. J. Morgan and L. A. Sazanov, unpublished observations). (C and D) Solvent-accessible surface area, colored red for negative, white for neutral, and blue for positive surface charges. Calculated with the APBS plug-in in PyMOL, using a sphere with a radius of 1.4 Å as a probe. The orientations are similar to those of panels A and B, respectively. N indicates the NADH-binding cavity and A the acidic grove between the C-terminal domain of Nqo3 and the rest of the complex.

Overall Architecture and Evolutionary Origins

The hydrophilic domain of *T. thermophilus* complex I consists of eight subunits (Nqo1−6, Nqo9, and Nqo15) with a combined molecular mass of 280 kDa (Figure 1). The domain has a specific overall Y shape, which can be discerned in some of the previously determined low-resolution electron microscopy (EM) structures. It is especially pronounced in the reconstructions of complex I from *Aquifex aeolicus* (*7*), *Neurospora crassa* (*16*), and *Yarrowia lipolytica* (*17*), and we have observed it with the bovine and *Escherichia coli* enzymes (D. J. Morgan and L. A. Sazanov, unpublished data). The Y shape was also visible in the earlier random conical tilt reconstruction of negatively stained bovine complex I (if the original assignment of the membrane and peripheral arms is reversed) but was lost in a nominally higher resolution structure obtained in ice (*6*). One of the reasons for this discrepancy may lie in the conformational flexibility of complex I in solution, as demonstrated recently for the *Yarrowia* enzyme (*17*). Many of the previous reconstructions are two-dimensional side views of the negatively stained enzyme, where Y shape features may be masked due to stain artifacts. Comparison with EM structures of the intact complex allowed us to suggest that the membrane domain extends in the direction of amphipatic

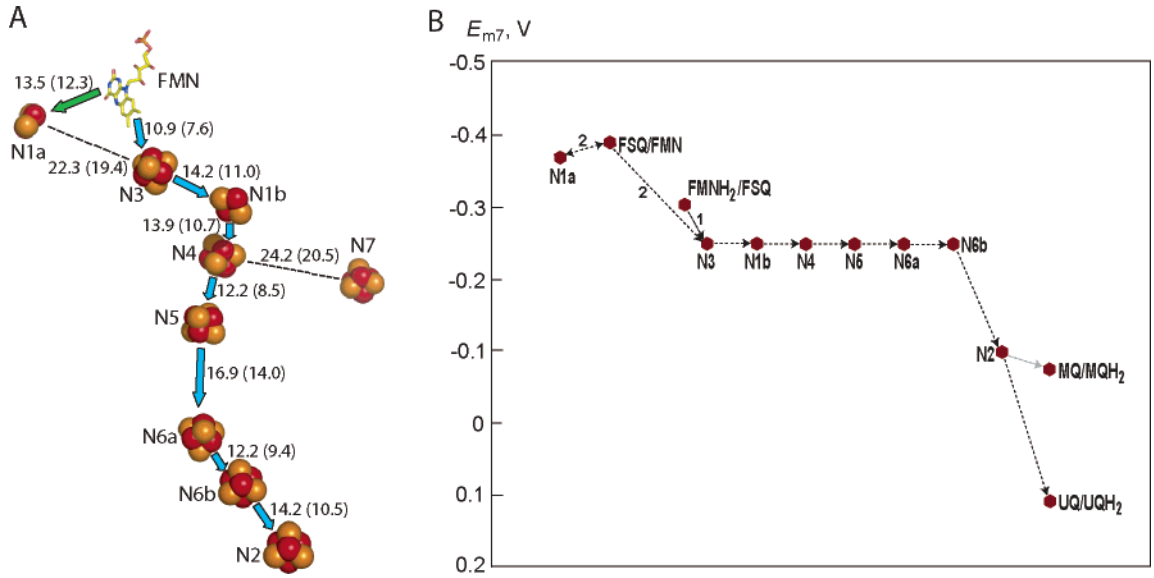

FIGURE 2: Spatial and redox potential distribution of redox centers. (A) Arrangement of redox centers. The overall orientation is similar to that of Figure 1A. The main pathway of electron transport is denoted with blue arrows, and a diversion to cluster N1a is denoted with a green arrow. The distances between the centers given in angstroms were calculated from both center to center and edge to edge (in parentheses). (B) Midpoint redox potentials, with average values at pH 7.0 as determined for the bovine and other enzymes (*2*, *13*). Two-electron potentials of quinone/quinol couples (both for ubiqinone, UQ, and for menaquinone, MQ, used by *Thermus*) are shown. For FMN, one-electron potentials for couples involving reduced $FMNH_2$, flavosemiquinone (FSQ), and oxidized FMN are shown. The numeral 1 denotes the first electron leaving the reduced flavin and the numeral 2 the second electron, leaving the flavin initially to cluster N1a for temporary storage and then to N3.

helix H1 from subunit Nqo6, which together with Nqo4 forms an interface with the membrane domain subunits (Figure 1A,B).

Most subunits of the complex, apart from Nqo5, are structurally homologous to soluble proteins, which apparently served as smaller "building blocks" during the evolution of the enzyme. These blocks, containing different redox centers, fit together perfectly in the structure in such a way that a continuous electron transfer pathway through the enzyme is formed. The evolutionary origins of complex I can thus be traced to different types of ferredoxins (subunits Nqo2 and Nqo9), FeFe-hydrogenases (N-terminus of subunit Nqo3), molybdopterin-containing enzymes (C-terminus of subunit Nqo3), and NiFe-hydrogenases (subunits Nqo4 and Nqo6). Such similarities were noted previously from sequence comparisons (*1*, *18*−*20*).

Many protein complexes with an as yet unknown structure seem to share the building blocks with complex I. Several NAD^+-reducing enzymes, for example, cytoplasmic NiFe-hydrogenase (*1*) and formate dehydrogenase (*21*) from *Ralstonia eutropha*, contain analogues of subunits Nqo1−3, the "dehydrogenase domain" of complex I. Membrane-bound NiFe-hydrogenases contain analogues of the "connecting domain" subunits (Nqo4−6 and Nqo9) and of most membrane domain subunits, which may be involved in proton pumping (*19*). Thus, the structure of the hydrophilic part of complex I will be useful in understanding the function of these enzymes also.

Electron Transfer Pathway

The electron transfer pathway can be traced unambiguously through the structure, starting from the NADH-binding site and FMN, continuing through the "wire" of seven iron−sulfur clusters, and terminating with cluster N2 (Figure 2A). At pH 7, the two-electron midpoint redox potential (E_m) of NADH is approximately −320 mV, that of FMN approximately −340 mV, and that of ubiquinone (UQ) approximately 110 mV [*Thermus* utilizes menaquinone (MQ), approximately −80 mV]. The one-electron potential of cluster N1a is approximately −370 mV and that of cluster N2 approximately −100 mV, and all the other clusters are isopotential at approximately −250 mV (*2*, *13*) (Figure 2B). In the main redox chain, cluster N3 accepts electrons from the flavin, while the high-potential cluster N2 reduces the quinone at the interface with the membrane domain. The proton-pumping stoichiometry of complex I has been measured mainly with the bovine enzyme using UQ as an acceptor (*22*). ΔE_m between NADH and UQ is ~430 mV. In the case of the NADH/MQ pair, ΔE_m is only 260 mV, so the question of whether the stoichiometry would be the same or lower can be posed. However, the available free energy is determined not only by midpoint redox potentials but also by the relative concentrations of reduced versus oxidized NADH and quinone. Thus, the actual redox potential difference at a complex I site in vivo could be similar in bovine, *Thermus*, and other species, despite different quinone types being used. In view of the high degree of sequence conservation of the core complex I subunits, it seems likely that the mechanism and stoichiometry of the enzyme would be similar in various species.

One of the puzzling questions about complex I is why it contains so many Fe−S clusters. One of the reasons probably lies in evolutionary origins, as the various building blocks of the enzyme need to be connected through redox centers. This results in a chain from FMN to cluster N2 that is approximately 95 Å long (Figure 2A). Unlike other clusters from this chain, cluster N1b appears to be redundant, as the edge-to-edge distance from cluster N3 to N4 is 13.8 Å, within

the physiological limit of 14 Å (*23*), thus bypassing N1b. This is shorter than the longest distance in the chain (14.0 Å between clusters N5 and N6a), so it should not be rate-limiting. In the calculation of the distance from N3 to N4, we included both Fe and S atoms from the clusters. Although this is currently accepted practice, from the available pool of data it is not yet entirely clear whether S atoms from clusters should be included in such calculations (P. L. Dutton, personal communication). It does not make significant differences in the calculation of distances for other clusters in the structure whether both Fe and S or only Fe atoms are considered. However, the N3 and N4 clusters are arranged in such a way that inclusion of only Fe atoms in their edge-to-edge distance calculation results in a distance of 15.8 Å, significantly longer than the physiological maximum. In this case, N1b would be an essential component of the redox chain. Mutations removing cluster N1b may allow us to differentiate between the two models (Fe−S or Fe only), since in a latter case the activity of complex I should be reduced dramatically.

Apart from clusters forming the main redox pathway, two clusters are too far from others to participate in direct electron transfer. Tetranuclear cluster N7 is not conserved and is found only in *T. thermophilus*, *E. coli*, and some other bacteria. It is coordinated in the C-terminal domain of Nqo3 by $_3$Cys^{256}, $_3$Cys^{259}, $_3$Cys^{263}, and $_3$Cys^{291} (the prefix indicates the subunit number) and is likely to be an evolutionary remnant from molybdopterin-containing enzymes, where the analogous cluster has a function in electron transfer (*24*). In complex I, the function of this cluster may be to stabilize the fold of Nqo3. Cluster N4, the cluster closest to N7, is 20.5 Å distant and is coordinated in a ferredoxin fold. In FeFe-hydrogenases, this fold contains the second tetranuclear cluster FS4A, normally absent in complex I. However, in sequences of Nqo3 subunits from *A. aeolicus*, *Campylobacter jejuni*, and *Helicobacter pylori*, cysteines equivalent to FS4A ligands are conserved (*25*). Therefore, it is likely that complex I in these species contains an additional Fe−S cluster. From the superposition of our structure with that of FeFe-hydrogenase [PDB entry 1feh (*26*)], it appears that this additional cluster would be positioned within 14 Å of both clusters N4 and N7, thus linking N7 to the main redox chain. In the microaerophiles *C. jejuni* and *H. pylori*, the complex I analogue lacks subunits Nqo1 and -2 and may possess an alternative electron input module (*25*). However, since cluster N7 is close to the former molybdopterin binding site, it is conceivable that in these species it accepts electrons from an unknown cofactor possibly bound in place of molybdopterin and passes them into the main redox chain via the additional cluster. In *A. aeolicus*, subunits Nqo1 and -2 have been identified as part of the complex (*7*). However, the genes for other complex I subunits are not organized in an operon, but they are scattered over several gene clusters, with several copies of many subunits (*27*). This may indicate some flexibility in complex I assembly. The role of the putative additional FS4A-like cluster in *A. aeolicus* and in microaerophiles remains to be established by further functional studies.

Cluster N1a and ROS Production

Binuclear cluster N1a is another cluster that is distal from the main redox chain. Unlike cluster N7, N1a is conserved in complex I from all species and so must be important functionally. We have suggested the possibility that N1a may play the role of an antioxidant, preventing excessive generation of reactive oxygen species (ROS) by complex I (*14*). FMN accepts two electrons simultaneously (as a hydride) from NADH and transfers them one at a time to one-electron carrier Fe−S clusters. The one-electron redox potential of N1a is too low for acceptance of the first electron from reduced $FMNH_2$, but it is suitable for acceptance of the second electron, from flavosemiquinone (Figure 2B). Thus, two electrons from flavin can be donated nearly simultaneously to two nearby clusters, N3 (first) and N1a (second). This mechanism will prevent any significant accumulation of the flavosemiquinone intermediate, which could otherwise react with oxygen, leading to ROS production. The flavin is exposed to the solvent at the deep end of the NADH-binding cavity (N in Figure 1C), whereas cluster N1a is shielded and so is suitable for such a temporary storage of electrons. The Fe−S clusters of complex I remain highly reduced during catalytic turnover (*28*, *29*). Oxidation of terminal cluster N2 by membrane-embedded quinone is a rate-limiting step (*29*), so electrons can move from N1a, via FMN, toward cluster N3 only when, and as soon as, N2 is re-oxidized. Flavosemiquinone formed during this transfer will be very short-lived, as the electron transfer between redox centers is several orders of magnitude faster than quinone binding and/or release (*30*) and the flavosemiquinone/FMN pair represents a small but unfavorable redox potential barrier in this pathway (Figure 2B).

If cluster N1a were absent, the main redox chain, consisting of an odd number of clusters (seven), would be filled quickly by NADH in two-electron steps and the last incoming electron would have to be retained on flavin until the quinol was released and a new quinone molecule bound so that N2 could be oxidized. During turnover, this would result in a flavosemiquinone radical being nearly always present and thus lead to a high rate of ROS production. If the number of clusters in the main chain was even (for example, six), N1a might be less important, but the advantage of nearly simultaneous electron transfer from flavin to two nearby clusters would be lost. The need to keep the total number of clusters in the redox chain even (seven plus one) may be another reason why cluster N1b is retained in complex I. It is likely that *A. aeolicus* complex I with its putative FS4A-like cluster will also have an even number of redox-linked clusters (nine plus one). There seems to be no example of complex I in which a FS4A-like cluster would be present without cluster N7, which would have led to an odd number of clusters in the chain (eight plus one). In complex II, a conserved heme *b*, like cluster N1a, is also not in the main redox pathway and is also a likely antioxidant (*31*). Heme *b*, together with three Fe−S clusters, also makes an even total number of redox centers in this enzyme. Recently, it was shown by pulse radiolysis studies that heme *b* is essential for nearly simultaneous transfer of a pair of electrons to ubiquinone (*32*). Thus, complex II appears to possess a similar mechanism for efficient coupling of two- and one-electron transfers, avoiding radical formation. In most species (with the exception of *E. coli*), cluster N1a of complex I, with its low potential, is not observed by EPR in the presence of excess NADH (*13*). However, EPR measurements are performed in most cases under equilibrium conditions and in the absence of membrane potential and so may not reflect

the in vivo turnover conditions accurately.

It is known that during reverse electron transport (NAD^+ reduction with quinol in the presence of proton-motive force) complex I produces at least 10 times more ROS than during the forward reaction (*33*, *34*). Addition of NAD^+ strongly inhibits ROS production by the bovine enzyme in both directions with an apparent K_i of ~10 μM (*35*), but for NADH oxidation, this value is ~1 mM (*36*). K_m values for NADH oxidation and for NAD^+ reduction are in the range of 10 μM (*35*, *37*). The reverse reaction, ROS generation, and the NADH:ferricyanide reaction are all inhibited by NADH with apparent K_i values of ~40−100 μM (*35*, *37*). ADP-ribose inhibits only forward electron transfer (*36*). On the basis of these and other kinetic observations, it was suggested that bovine complex I has two distinct nucleotide-binding sites, one operating during NADH oxidation and another during NAD^+ reduction and ROS production (*35*). However, there is no evidence for a second functional nucleotide binding site in the *Thermus* structure. Most (or all) of the kinetic observations can be explained if we consider that the binding affinities for NAD(H) depend on the reduction state of the enzyme and the flavin. This is quite likely to be due to the close interaction between the nicotinamide ring and the flavin, although conformational changes near the binding site may also be involved. Such a dependence has been observed for various flavoenzymes; for example, the affinity of cytochrome P450BM3 for $NADP^+$ increases many-fold when the enzyme is reduced (*38*). Indeed, the protein surface is clearly positively charged around the nucleotide-binding site in complex I (N in Figure 1C), which will attract a negatively charged NADH molecule, but may be unfavorable for NAD^+ binding. However, when the flavin is reduced, there will be a negative shift in charge distribution and NAD^+ could bind more effectively. From comparisons of all available data (*35*−*37*), it is likely that the affinity of complex I for NADH is ~10 μM when the flavin is oxidized and ~100 μM when it is reduced, whereas the affinity for NAD^+ is ~1 mM when the flavin is oxidized and ~10 μM when it is reduced. Then the kinetic differences between the forward and reverse reactions are readily understood. These different affinities are also appropriate for the physiological reactions, as the flavin should be oxidized before it can accept electrons from NADH and should be reduced before it can pass electrons onto NAD^+. The unidirectional effect of ADP-ribose can also be due to the lower affinity of this inhibitor for the reduced enzyme. If the NADH:ferricyanide reaction proceeds via a ping-pong mechanism, it would be inhibited by NADH competing with ferricyanide for binding to the reduced enzyme, which is consistent with the proposal given above.

The flavin is bound at the deep end of a solvent-exposed cavity, containing an apparent nucleotide-binding site. When the nucleotide is bound, the flavin is likely to be protected from the solvent, as indicated by manual docking of NADH (not shown). Therefore, ROS may be produced only when the flavin is partly or fully reduced and nucleotide is absent, allowing the flavin to interact with dissolved oxygen. It has been reported recently that in such a mechanism, fully reduced flavin is responsible for ROS production (*39*). The presence of flavosemiquinone is likely to be minimal due to cluster N1a, as discussed above. The observed patterns of inhibition of ROS production by NAD^+ and NADH (*35*) are fully consistent with the apparent affinities of nucleotides for the reduced enzyme, as suggested above. Furthermore, in the reverse reaction, the binding of NAD^+ is likely to be preceded by flavin reduction, due to a low affinity of NAD^+ for the oxidized enzyme. Therefore, a significant proportion of reduced flavin would then be present in an empty active site, resulting in the observed high rates of ROS production. Inhibition of the forward reaction by rotenone often leads to high rates of ROS production (*34*), probably because of the increased level of reduced flavin, which cannot be oxidized by complex I under these conditions.

The inhibition of ROS production by complex I might limit mtDNA damage and thereby help in the treatment of some neurodegenerative diseases, such as Parkinson's, and possibly lead to increased longevity in humans. Clearly, such an inhibitor would be of great interest, provided that it does not inhibit normal complex I activity. From the mechanisms discussed above, a good candidate for such an inhibitor could be a nucleotide analogue which binds to the NADH site in complex I with an affinity intermediate between those of NADH and NAD^+, preventing exposure of FMN to the solvent. The fold around the NADH site in complex I is unique and differs from those of other dehydrogenases (*15*) and so might allow the development of a specific compound.

Coupling between Electron Transfer and Proton Translocation

Another important mechanistic question about complex I is how electron transfer is coupled to proton translocation. To answer this question, we need to determine the structure of the entire complex, preferably in several conformations. However, some clues can be gained from the structure of the hydrophilic domain (*15*). From two alternative views, direct (redox-linked) versus indirect (conformationally linked) coupling (*2*), a support for direct coupling, via some chemical intermediate, may be inferred from the location of the invariant $_4Tyr^{87}$. It is near cluster N2 and faces the quinone-binding site (Q-cavity), found at the interface of subunits Nqo4 and Nqo6 and the membrane domain (*15*). This tyrosine is essential for activity (*40*) and could participate in both electron and proton transfer. The unique coordination of terminal cluster N2 by two conserved consecutive cysteines is also notable. Previously, this was thought to be impossible due to steric constraints, even though mutagenesis indicated otherwise (*41*). More recently, the feasibility of such coordination was suggested on the basis of molecular modeling (*42*), although the proposed fold was not similar to the one later found in the structure. This unusual coordination could in principle allow direct protonation of the cluster upon reduction, leading to the observed pH dependence of its potential (redox-Bohr effect). However, it was reported recently that $_4His^{169}$, which is hydrogen-bonded to N2, seems to be responsible for the redox-Bohr effect (*43*). FhuF, a siderophore-iron reductase from *E. coli*, contains an atypical [2Fe-2S] cluster, apparently also coordinated by two consecutive cysteines (*44*). Methanol dehydrogenase contains, in its active site, an unusual disulfide bond formed between two consecutive cysteines, resulting in a strained local conformation (*45*). Possibly, the unusual coordination of N2 in a rather unfavorable conformation allows higher flexibility of the fold around the cluster, which

may be important for the mechanism, particularly for any related conformational changes.

Simple variations of the Q-cycle type of direct coupling mechanism cannot account for as many as four protons pumped for each NADH oxidized. On the other hand, it is known that both *E. coli* complex I (*46*) and bovine complex I (*47*) change conformation significantly upon reduction with NADH. Kinetic studies indicated that binding of NADH to the bovine enzyme results in a conformational change at the quinone-binding site (*48*). Complex I contains in its membrane domain three similar subunits, Nqo12−14, homologous to the monovalent cation/proton antiporters and therefore likely to be involved in proton translocation. The spatial separation between the electron transfer pathway and at least two of these subunits, Nqo12 and -13, also points to the possibility of indirect, conformational coupling in complex I (*49*−*51*). Several features of the structure support this proposal. The conserved helix H2 extends away from subunit Nqo4 and interacts via charged residues with clusters N5 and N6a (Figure 1A and Figure 2F in ref *15*). Since these clusters are separated by the longest distance in the redox chain (Figure 2A), they are likely to be the most sensitive to the redox state of the enzyme. Helix H2 may provide a way to communicate the redox state of these clusters to the membrane domain, through conformational changes. A very long four-helix bundle in Nqo4 (residues 107−320; Figure 2F in ref *15*) could participate in this communication, as it is roughly between H2 and the membrane domain. A good analogy is provided by the Ca^{2+}-ATPase, which undergoes large conformational changes during its catalytic cycle, where rearrangements of cytosolic domains are linked to movements of transmembrane helices, resulting in Ca^{2+} translocation (*52*, *53*). This connection is made in part through a helical bundle, an extension of some of the TM helices. Amphipatic helix M1′ moves onto the membrane surface during these conformational changes (*52*).

In complex I, amphipathic helix H1 extends, most likely on the surface of the membrane domain, away from subunit Nqo6 toward antiporter-like subunits Nqo12−14. This 25 Å long helix is predicted to extend for another 10 residues at the N-terminal part [PredictProtein server (*54*)], not resolved in the structure. Helix H1 is linked to cluster N2 via a β-strand, and its C-terminus interacts with the C-terminus of another α-helix (residues 143−160 of Nqo6), also linked to cluster N2 at ${}_6Cys^{140}$. This arrangement may also provide a conformational link between the distal (proton-pumping) subunits Nqo12−14 and Fe−S clusters, in particular N2, with helix H1 acting as a kind of "lever" in the proton pump. Additionally, the helix directly involved in cluster N2 coordination (residues 45−55 of Nqo6) extends from N2 into the membrane domain area and may also be a part of the coupling mechanism. Consistent with these proposals, we have observed by cross-linking studies that Nqo6 is the most mobile subunit during the transition from the oxidized to the NADH-reduced form of the *E. coli* enzyme (*46*).

To account for four protons being pumped during one catalytic cycle, and on the basis of the modular organization of subunits in the enzyme, it was proposed previously that a combination of direct and indirect mechanisms might operate in complex I (*50*, *55*, *56*). For such a mechanism, it seems logical to suggest that a direct coupling site, formed around the Q-cavity at the Nqo4−Nqo6 interface, is responsible for one pumped proton, with the three other protons being pumped, one each, by the three antiporter-like subunits Nqo12−14 driven by conformational changes. Further structural work should resolve these issues.

Below, a number of structural features of individual subunits are described that have not been discussed previously (*15*), together with significant effects of known mutations. Many of the mutations were discovered by being associated with human diseases, whereas others were created in model systems either to study these diseases or to investigate conserved residues of functional interest. The summary of known mutations in conserved hydrophilic subunits of complex I, with the explanation of the effects based on the structure, is given in Table 1. Most mutations of surface-exposed residues (for example, ${}_6Asp^{128}$, ${}_6Asp^{134}$, ${}_6Y^{136}$, or ${}_5R^{147}$) have a mild effect on the activity or on other properties of the enzyme, whereas most mutations close to the redox centers or to substrate-binding sites have severe consequences. Thus, most of the effects can be explained readily, suggesting that the *T. thermophilus* structure can be used as a good model of complex I in humans and other species. The mutations of particular interest are discussed in more detail below.

Individual Subunits and Known Mutations

Nqo1/51 kDa/NDUFV1 (Thermus/bovine/human nomenclature). Subunit Nqo1 contains the primary electron acceptor FMN at the deep end of a solvent-exposed cavity (the NADH binding site). Apart from cluster ligands, only one cysteine residue, ${}_1Cys^{182}$, is conserved in complex I. It is located only 6 Å from the FMN, and it can also interact with it via the neighboring ${}_1Gly^{183}$, which is hydrogen-bonded to the isoalloxazine ring. This cysteine has been identified as a redox-sensitive thiol and as the site of oxidative attack by ROS generated by NADH-reduced complex I (*57*). This is consistent with the possibility of ROS production by the flavin. Notably, ${}_1Cys^{182}$ is within hydrogen bonding distance of the hydroxyl of ${}_1Tyr^{133}$ (a semiconserved residue) and is within 4 Å of ${}_2Tyr^{67}$ (an invariant residue). The chain of ionizable residues, all within 4 Å of each other (Figure 3), is then continued from ${}_1Tyr^{133}$ to the protein surface, via ${}_1His^{174}$ (semiconserved), ${}_2Tyr^{18}$ (semiconserved), ${}_1Tyr^{131}$ (semiconserved), ${}_1His^{172}$ (not conserved, surface-exposed), and ${}_1Arg^{153}$ (not conserved, surface-exposed). In bovine complex I, the residue corresponding to ${}_1Arg^{153}$ (Tyr177) was identified as another specific site of oxidative attack (*57*). Therefore, it seems plausible that this chain of ionizable residues may provide a link between FMN and the protein surface, as a pathway for electrons to escape from flavin when the NADH site is occupied and the clusters are reduced. This may happen when either the quinone pool is highly reduced or complex I is inhibited. Alternatively (or additionally), this chain of residues could provide a way of communicating the redox state in the cell to the flavin site. The simultaneous mutation of ${}_1Cys^{182}$ and ${}_1Tyr^{180}$ has severe consequences (Table 1), which can be explained by these residues being near the FMN and by a probable role of ${}_1Tyr^{180}$ as a NADH ligand (*15*).

One of the novel features of the Nqo1 fold was the coordination of cluster N3 within a four-helix bundle (*15*).

It has been noted previously that the motif binding N3 cluster "CxxCxxCx$_{40}$C" is strikingly conserved not only in complex I but also in a variety of hydrogenases and dehydrogenases (*58*). Thus, these enzymes are likely to coordinate a cluster in a similar four-helix bundle, a structural motif that was not known previously to bind Fe−S clusters.

Nqo3/75 kDa/NDUFS1. The structure clearly shows that cluster N5 is coordinated by three cysteines and a histidine ($_3$His^{115}). This arrangement is consistent with studies on the Nqo3 subunit from *Paracoccus denitrificans*, where mutations to the $_3$His^{115} analogue specifically affected cluster N5 (*59*). However, in a later study with the *Y. lypolityca* enzyme (*60*), mutation of the respective histidine to alanine seemingly did not affect cluster N5, but NADH:quinone activity was completely abolished. One possible explanation for this apparent discrepancy could be that the EPR signal for cluster N5 has been incorrectly assigned in *Y. lypolityca.* It is feasible that the signal from cluster N2 shifts slightly to higher g_z values at low temperatures and a high microwave power, giving rise to an apparent N5 signal (*60*, *61*). If cluster N5 was indeed removed, a gap of ∼25 Å in the redox chain would be created (edge-to-edge distance between clusters N4 and N6a in our structure), consistent with the total loss of activity. Alternatively, it is possible that after the mutation cluster N5 in *Y. lypolityca* is still coordinated by the three remaining cysteines. However, some change in EPR properties would have been expected, and it is more difficult then to explain the complete loss of activity.

One of the notable mutations in Nqo3 is the change of conserved leucine 235 to valine, which in humans leads to infant death and a large decrease in enzyme activity (Table 1). The drastic effects of this seemingly conservative change are readily explained by the structure: $_3$Leu^{235} is within hydrogen bonding distance of cluster N4, so the mutation is likely to change the redox potential and/or destabilize the cluster.

The role of the large C-terminal domain of Nqo3 (residues 241−767), which does not contain any conserved cofactors and does not interact directly with other subunits, is not clear at the moment. One possibility is that it may be involved in any mechanistically important conformational changes. The domain contains cluster N7 and the ancestral molybdopterin guanine dinucleotide (MGD)-binding site, inherited from MGD-containing enzymes (*15*). This site (having lost its molybdopterin cofactor during evolution) is capped by subdomain IV (residues 671−767). However, a relatively long (15 Å) but quite narrow (∼2 Å minimal cross section) solvent-accessible cavity or channel remains, reaching from the surface (near $_3$His^{591} and $_3$His^{589}) to $_3$Glu^{353} and $_3$Asp^{348} at the bottom (Figure 4). The cavity is also lined by tyrosine 567 and up to four additional histidines (347, 586, 702, and 757). The surface charge in the cavity is negative at the bottom and near the entrance, but positive in the middle, resembling the charge distribution in the putative Fe-binding channel formed at the interface with subunit Nqo15 (*15*). All these properties seem to be appropriate for binding metal cation(s) at the bottom of the cavity, possibly coordinated by $_3$Glu^{353}, $_3$Asp^{348}, and some of the histidines. The positive charge in the middle of the cavity may prevent the cation from escaping once it is bound at the deep end. When Nqo3 is superimposed with subunit NarG from respiratory nitrate reductase (PDB entry 1R17), $_3$Asp^{348} is only 4 Å from Asn52 of NarG, which is also found at the bottom of a cavity and is implicated in substrate binding (*62*). Bovine complex I is inhibited by divalent cations (Zn^{2+}, Cd^{2+}, Mg^{2+}, and Ca^{2+}, among others), and the degree of inhibition appears to depend on the conformational state of the enzyme (*63*, *64*). The cavity shown in Figure 4 could be one of the sites involved in such inhibitory effects.

The entrance to this cavity is near the extensive surface area with a prominent negative charge (A in Figure 1D). This area, or "acidic groove", is located between the C-terminal domain of Nqo3 and the rest of the complex. One possible role of such an unusual charge distribution could be to attract ions to the putative cation binding site near $_3$His^{591}. Alternatively, it is conceivable that some as yet unknown protein partner with a positive surface charge interacts with complex I in this area. Another proposal is that it may be important for interaction with Nqo3 subdomain IV if the lid, formed by it, opens during any conformational changes (*15*, *46*) and perhaps moves toward this negatively charged area. In the human enzyme, mutation of Gln522 to Lys (corresponding in *Thermus* to $_3$Ala^{541}, located near the former MGD site) leads to the formation of an ∼800 kDa subcomplex, to an 80% decrease in activity, to an increased affinity for NADH, and to overproduction of ROS (*65*). All of these effects appear to be consistent with the possible participation of the C-terminal domain of Nqo3 in a conformational coupling mechanism, as the domain is not in direct contact with substrate-binding sites.

During apoptosis, it has been suggested that caspases (acting in the intermembrane space) cleave a site in the 75 kDa subunit of human complex I (*66*). From sequence alignments, this site corresponds to the area around cluster N7 in Nqo3 (residues 256−259, including two N7 cysteine ligands). As the mitochondrial intermembrane space and the bacterial periplasm are topologically equivalent, it is highly unlikely that the proposed caspase site can protrude all the way to and through the membrane. Therefore, the mode of action of caspases on complex I needs to be re-evaluated.

Nqo4/49 kDa/NDUFS2 and Nqo6/PSST/NDUFS7. These two subunits interact extensively and are discussed together. The position of the essential $_4$Tyr^{87}, within 8 Å of cluster N2, is consistent with the effects of its mutation to histidine, which lead to the broadening of the EPR signal and to a shift of the g_z value for N2 (*40*). Mutations of other residues in the vicinity of N2 also altered EPR signals of this cluster (Table 1). Apart from $_4$Tyr^{87}, several other conserved residues, also lining the Q-cavity, have been mutated. In most cases, the mutations lead to a significant decrease in quinone reductase activity and to changes in sensitivity to quinone-like inhibitors (Table 1), consistent with our proposal for the Q-site being formed at the interface of Nqo4, Nqo6, and the membrane domain.

Conserved $_6$Asp^{76} is near the protein surface, but it is hydrogen-bonded to the backbone amide of $_6$Trp^{37} at the C-terminus of helix H1. Mutations of this residue reduced the activity dramatically, which may be due to the possible role of helix H1 in the coupling mechanism, as discussed above. Another conserved residue, $_4$Glu^{51}, although exposed at the surface of the isolated hydrophilic domain, faces toward the interface with the membrane domain and is likely to interact with hydrophobic subunits. This arrangement may explain the severe consequences of its mutation (Table 1).

Table 1: Mutations in the Conserved Hydrophilic Subunits of Complex I and Interpretation of Observed Effects, Based on the Structure of the Hydrophilic Domain of Complex I from *T. thermophilus*[a]

species, mutation	residue in *T. thermophilus*	ref(s)	activity (%)	human disease, if associated with the mutation	effects of mutations in humans or in the model organism[b]	explanation based on the structure
				Nqo1/51 kDa/NDUFV1		
Caenorhabditis elegans						
A352V	H315	*75*, *76*	37	hypotonia, ataxia, infant death	R, premature aging, oxidative damage	surface, near NADH site
T434M	S398	*75*, *76*	52	hypotonia, ataxia, infant death	R, premature aging, oxidative damage	4.1 Å from cluster N3
A443F	V407	*75*, *76*	23	hypotonia, ataxia, infant death	R, premature aging, oxidative damage	interface between helices from cluster N3 fold
N. crassa						
A353V	H315	*77*	0	hypotonia, ataxia, infant death	subunit degraded	surface, near NADH site
T435M	S398	*77*	55	hypotonia, ataxia, infant death	R	4.1 Å from cluster N3
human						
Y204C/C206G	**Y180** and **C182**	*78*	18	hypotonia, ataxia, infant death		Y180 - possible NADH ligand; C182 is 6 Å from FMN, linked through a chain of Tyr and His residues to $_1R^{153}$ on the surface
E214K	N190	*78*	57	hypotonia, ataxia, infant death		interface with Nqo3
				Nqo2/24 kDa/NDUFV2		
Y. lipolytica						
deletion of codons 17−32, part of presequence	not present	*79*	100	cardiomyopathy and encephalomyopathy	normal activity, residual presequence retained	N-terminus of Nqo2 is on the surface of the complex
				Nqo3/75 kDa/NDUFS1		
Y. lipolytica						
H129A	**H115**	*60*	<3		R, U, cluster N5 still present?	cluster N5 ligand
P. denitrificans subunit expressed in *E. coli*						
H106C/H106A	**H115**	*59*	n/a		cluster N5 altered; all clusters not incorporated	cluster N5 ligand
human						
Δ**I222**/D252G	**I226** and C256	*78*	67	hypotonia, ataxia, infant death		I226 is 4 Å from $_3C^{187}$ (cluster N4 ligand); C256 is cluster N7 ligand
L231V	**L235**	*80*	25	Leigh syndrome, infant death		3.6 Å from cluster N4
R241W	**R245**	*78*	77	hypotonia, ataxia, infant death		between clusters N5 and N6a, H-bond to $_3C^{119}$ (cluster N5 ligand)
Q522K	A541	*65*	20	encephalopathy	formation of ∼800 kDa subcomplex; increased level of ROS production, affinity for NADH	interior, facing former molibdopterin-binding cavity
M707V	E744	*78*	50	hypotonia, ataxia, infant death		surface, salt bridge to $_3R^{713}$
				Nqo4/49 kDa/NDUFS2		
Y. lipolytica						
F87L	V30	*81*	59	Leigh syndrome	QR	not in the structure
H91AMR	**H34**	*82*	<5			not in the structure
H95AMR	**H38**	*82*	<5			lining Q-cavity near $_4Y^{61}$, to the side of the complex
E107A	**E51**	*81*	<5	Leigh syndrome		interface with the membrane domain
H120A	**H63**	*40*	39			near surface, H-bond to $_6Y^{121}$; through backbone oxygen H-bond to $_6R^{83}$, which is H-bonded to cluster N2
R141A	**R84**	*40*	17		N2N	H-bond to cluster N2
R141K	**R84**	*82*	45		N2R, QR	H-bond to cluster N2
R141M			40		N2N	
D143E	**D86**	*40*	23		QR, N2A	near Q-cavity; H-bond to $_4R^{350}$ (lining Q-cavity); 12 Å from cluster N2
D143C			30		QR	
Y144H	**Y87**	*40*	<5		N2A	lining Q-cavity, 4 Å from $_6C^{45}$ (cluster N2 ligand)
H226A	**H169**	*40*	25		N2N	H-bond to cluster N2
H226Q	**H169**	*82*	56		N2R	H-bond to cluster N2

Table 1 (Continued)

species, mutation	residue in *T. thermophilus*	ref(s)	activity (%)	human disease, if associated with the mutation	effects of mutations in humans or in the model organism[b]	explanation based on the structure
			Nqo4/49 kDa/NDUFS2 (Continued)			
H226C			43		N2R	
H226M			80		N2A, QS	
R231Q	**R174**	*81*	101	Leigh syndrome	some QR	interior, salt bridge to $_9$E^{106}, 8 Å from $_9$C^{101} (cluster N6b ligand)
R231E			74		some QR	
P232Q	I175	*81*	17	Leigh syndrome	R, U	interior, near interface with Nqo3
P232G			56		R	
H384A	**H327**	*40*	47			interior, H-bond to the backbone oxygen of $_9$C^{108} (cluster N6a ligand)
S416P	**S359**	*81*	111	Leigh syndrome	QR	interior, H-bond to the backbone oxygen of $_4$P^{337}, stabilizing β-sheet
S416A			86			
D458A	**D401**	*40*	28		QR	lining Q-cavity
V460A	**V403**	*40*	<5		N2N	lining Q-cavity, next to $_4$Y^{87}, 11 Å from N2
V460M			28		QR, N2R	
E463Q	**D406**	*40*	20		R, QR, N2R	near Q-cavity, 14 Å from N2
R466A	**R409**	*82*	75		R, U, N2R, QR	salt bridge to $_5$D^{120}
R466M			9		R, U, N2R	
R466H			85		QR, increased K_m for DBQ	
R466E			53		R, U, N2R	
Rhodobacter capsulatus						
D405E	**D401**	*83*	50			lining Q-cavity
V407M	**V403**	*83*	50		QR	lining Q-cavity, next to $_4$Y^{87}, 11 Å from N2
V407L			50			
G409A	**G405**	*83*	20		QR	near Q-cavity, 4 Å from $_4$Y^{87}
D412E	**D408**	*83*	50		QR	interior, 6 Å from Q-cavity
R413K	**R409**	*83*	30			salt bridge to $_5$D^{120}
			Nqo5/30 kDa/NDUFS3			
Y. lipolytica						
T157I	V92	*81*	90	Leigh syndrome, mild		interior, in β-sheet, facing helix
R211W	**R147**	*81*	90	Leigh syndrome, mild		surface, H-bond to $_5$D^{149}
			Nqo6/PSST/NDUFS7			
Y. lipolytica						
E89Q	**E49**	*84*	88		N2A	7 Å from cluster N2; lining Q-cavity, H-bond to $_4$R^{167}
E89C			67		N2A	
E89A			74		N2A	
D99N	**D59**	*85*	<5		U, N2R	not in the structure, likely in the loop at the membrane domain interface
D99E			<5			
D99G			<5			
D115N	**D76**	*85*	6		U, N2R	at the membrane domain interface, H-bond to $_6$W^{37} at the C-terminus of helix H1
D115E			5		U	
D115G			6			
V119M	**V80**	*86*	50	Leigh syndrome	QS, decreased K_m for DBQ, N2R	interior, 9 Å from $_6$C^{46} (N2 ligand)
D136N	**E97**	*84*	17		sensitive to rotenone, resistant to DQA	surface, near Q-cavity and the membrane domain interface
E140Q	**D101**	*84*	47		sensitive to rotenone, resistant to DQA	surface, near helix H1 and the membrane domain interface
D168N	**D128**	*84*	97			surface, possible H-bond to $_6$Y^{136}
D174N	**D134**	*85*	100			near surface, H-bond to $_6$K^{157}
E185Q	**E145**	*85*	35		increased K_m for DBQ	surface, near Q-cavity and the membrane domain interface

Table 1 (Continued)

specied, mutation	residue in *T. thermophilus*	ref(s)	activity (%)	human disease, if associated with the mutation	effects of mutations in humans or in the model organism[b]	explanation based on the structure
			Nqo6/PSST/NDUFS7 (Continued)			
N. crassa						
V135M	**V80**	*77*	43	Leigh syndrome	R	interior, 9 Å from $_6$C^{46} (cluster N2 ligand)
E. coli						
E67Q	**E49**	*87*	10		R, N2R, and N2 midpoint potential shifted by −30 mV	7 Å from cluster N2; lining Q-cavity, H-bond to $_4$R^{167}
E67D			78		N2R	
D77N	**D59**	*87*	12		R, slightly unstable, N2R	not in the structure, likely in the loop at the membrane domain interface
D77E			54		R, N2R	
D94N	**D76**	*87*	12		R, U	at the membrane domain interface, H-bond to $_6$W^{37} at the C-terminus of helix H1
D94E			83		R, U	
D115N	**E97**	*87*	45			surface, near Q-cavity and the membrane domain interface
E119Q	**D101**	*87*	88			surface, near helix H1 and the membrane domain interface
D146N	**D128**	*87*	59		R	surface, possible H-bond to $_6$Y^{136}
D152N	**D134**	*87*	59		R	near surface, H-bond to $_6$K^{157}
E163Q	**E145**	*87*	76		R	surface, near Q-cavity and the membrane domain interface
Y114C	W96	*67*	100		N2A	near surface, 20 Å from cluster N2
Y139CF	**Y121**	*67*	100		N2A	near surface, 16 Å from cluster N2, H-bond to $_4$H^{63}
Y154HF	**Y136**	*67*	100		N2A	near surface, 15 Å from cluster N2, possible H-bond to $_6$D^{128}
Y114C/**Y139F**	W96 and **Y121**	*67*	20		U, N2R, FTIR spectra affected	near surface, 20 Å from cluster N2; near surface, 16 Å from cluster N2, H-bond to $_4$H^{63}
			Nqo9/TYKY/NDUFS8			
Y. lipolytica						
P98L	**P21**	*86*	57	Leigh syndrome		not in the structure
R121H	T44	*86*	45	Leigh syndrome	QS	7 Å from $_9$C^{108} (N6a ligand)
N. crassa						
R111H	T44	*77*	34	Leigh syndrome	R, N2R, U	7 Å from $_9$C^{108} (N6a ligand)
Rh. capsulatus						
E71K	A60	*88*	33			7 Å from both N6a and N6b

[a] Fully conserved residues are shown in bold. This includes conservative changes between Asp and Glu. Mutations to Cys ligands of Fe−S clusters are not discussed here, as the interpretation is usually straightforward. "Not in the structure" means that this residue was not modeled due to poor electron density. Prefixes to residue names indicate the subunit number. [b] Abbreviations: R, reduced amount of complex or individual subunits; U, unstable complex; QR, increased resistance to Q-like inhibitors; QS, increased sensitivity to Q-like inhibitors; N2A, altered cluster N2; N2R, reduced amount of cluster N2; N2N, cluster N2 not observed; DBQ, *n*-decylbenzoquinone, substrate analogue; DQA, 2-decyl-4-quinazolinyl amine, ubiquinone-like inhibitor; Q-cavity, a cavity containing the likely quinone-binding site at the interface of subunits Nqo4 and Nqo6 and the membrane domain.

On the basis of FTIR spectroscopy, it has been suggested that tyrosine residues 114 ($_6$Trp^{96} in *Thermus*) and 139 ($_6$Tyr^{121}) from the NuoB subunit in *E. coli* are protonated when cluster N2 is reduced, as part of a proton pumping mechanism (*67*). However, in the structure, $_6$Trp^{96} is exposed to the outside surface of the complex, whereas $_6$Tyr^{121} is located to the side from cluster N2, away from the membrane interface, and so is in an inappropriate position to be directly involved in proton pumping. Nevertheless, this invariant $_6$Tyr^{121} is hydrogen-bonded to invariant $_4$His^{63}, and the hydrogen bond network then continues via the backbone carbonyl to $_6$Arg^{83} and cluster N2. Thus, protonation of $_6$Tyr^{121} may be linked to the redox state of N2, but only as a part of an indirect, possibly conformational coupling. It was also suggested from FTIR spectroscopy that the oxidation of cluster N2 is coupled with the protonation of the side chain of an aspartate or glutamate residues (*68*). There are several highly conserved acidic residues lining the Q-cavity, which are potential candidates for such protonation if it is a part of coupling mechanism, namely, $_4$Asp^{139}, $_4$Glu^{154}, $_4$Glu^{161}, $_4$Asp^{401}, $_6$Glu^{49}, and $_6$Glu^{145}.

Nqo15. This novel subunit has a fold similar to the unique fold of the frataxins, which are iron chaperones. It forms a possible iron-binding channel at the interface with the rest of complex (*15*). Homologous proteins are found in *Deinococcus radiodurans* and *Deinococcus geothermalis* (*5*), close relatives of *T. thermophilus*, where they are likely to form a part of complex I also, but not in other species. Thus, the

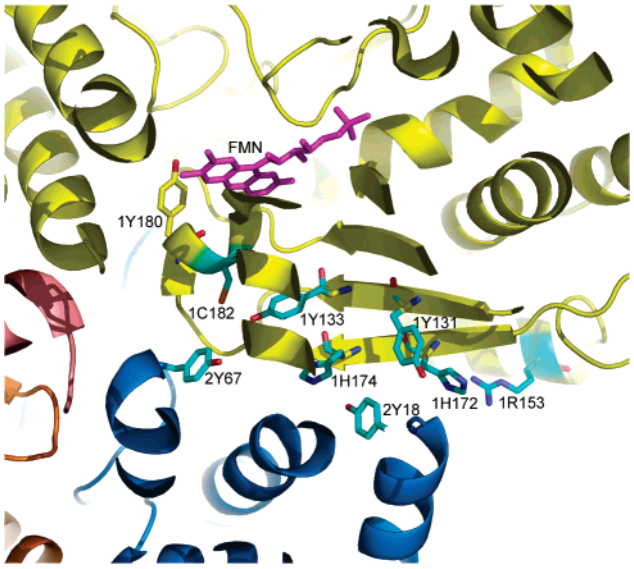

FIGURE 3: Environment of the invariant cysteine residue, $_1$Cys^{182}. Ionizable residues forming a putative link between $_1$Cys^{182} and the protein surface are colored cyan. Prefixes to residue names indicate the subunit number.

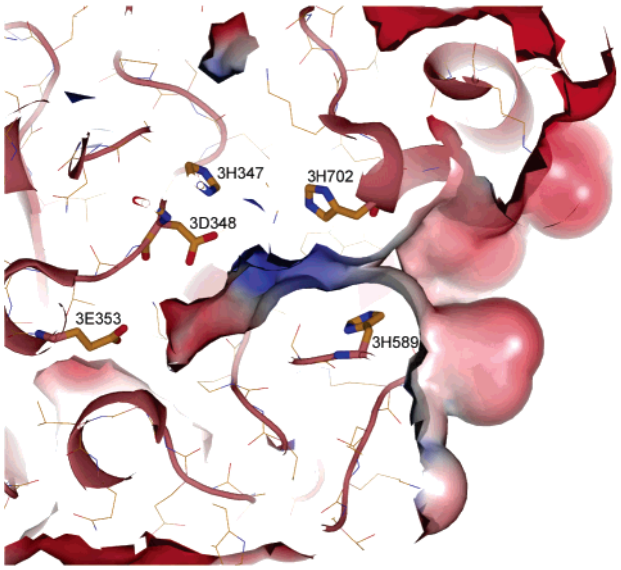

FIGURE 4: Possible cation-binding cavity in the C-terminal domain of Nqo3. Residues that could be involved in binding or delivery of the cation to the binding site at the bottom of the cavity are shown. Prefixes to residue names indicate the subunit number.

Nqo15 subunit appears to be unique to complex I from a restricted number of thermophiles. However, despite the very high degree of similarity of the Nqo15 fold to frataxins (rmsd $\sim$ 2.5−3.0 Å), the degree of sequence conservation is low [11−13% identical (*15*)] and cannot be detected by BLAST or similar search algorithms. Therefore, it is possible that a structural and functional analogue of Nqo15 could be present in complex I from other species, but it escaped detection so far due to a low degree of sequence similarity.

Genes for bona fide frataxins in sequenced genomes usually occur jointly with genes from the Isc (iron−sulfur cluster assembly) operon (*69*). One of the functions of frataxins is thought to be the delivery of iron for the Isc machinery during Fe−S cluster assembly (*70*). In *T. thermophilus*, however, even though Isc proteins are present, there is no clear frataxin analogue in the genome. It is possible that Nqo15 may play a double role in *Thermus*, both as part of complex I and as a soluble frataxin analogue. Alternatively, there may be another frataxin analogue in *Thermus*, but with a low degree of sequence similarity to known frataxins.

At the negatively charged bottom of the channel formed by Nqo15, there is a putative Fe-binding site (as suggested by frataxin similarity) formed by $_{15}$His^{92}, $_3$His^{208}, and $_3$Glu^{204}. The arrangement of residues is very similar to that in the 2-His-1-carboxylate facial triad motif found in various Fe(II)-binding enzymes (*71*). Frataxins also bind Fe(II) (*72*). Apart from conserved His^{92}, Nqo15 contains two conserved histidines at positions 94 and 96, which are well-positioned within the channel to act as anchors delivering Fe from the solvent to the triad motif site. $_3$His^{208} is conserved, for example, in *D. radiodurans*, *D. geothermalis*, *A. aeolicus*, and *Rhodospirillum rubrum* and is replaced with Asp in *Sinorhizobium meliloti*, *Paracoccus denitrificans*, and the bovine enzyme. $_3$Glu^{204} is conserved in *D. radiodurans*, *D. geothermalis*, *S. meliloti*, and *Mycobacterium tuberculosis* and is replaced with Asp in *A. aeolicus*. Thus, a similar Fe-binding motif is most likely to exist in *D. radiodurans* and *D. geothermalis* and may also be found in *A. aeolicus* and some other species if they contain an Nqo15 analogue. If iron is indeed stored at this site, it could be used for the regeneration of nearby clusters N3 ($\sim$11 Å away) and N1a ($\sim$18 Å away).

In addition to the facial triad motif, there could be a second putative Fe-binding site slightly to the side of the channel, formed by $_2$Glu^{123}, $_1$His^{350}, and $_1$Glu^{351}. This site is only 8 Å from cluster N1a, but it is $\sim$10 Å from cluster N3 and so could be used preferentially for regeneration of N1a. Residue $_1$Glu^{351} is invariant, whereas $_2$Glu^{123} is conserved mostly in the same species as $_1$His^{350}, including *D. radiodurans* and *D. geothermalis*.

Most invariant residues from frataxins are not conserved in Nqo15. However, some conservation is observed around putative Fe-binding sites. NMR studies of binding of Fe to the bacterial frataxin analogue CyaY indicated that initially iron binds to several acidic residues exposed at the surface of the N-terminal helix (including glutamates 19 and 5), and then, with increasing Fe concentrations, to several residues (including Asp72) corresponding in Nqo15 to those exposed inside the channel (*70*). These residues are conserved in Nqo15. $_{15}$Glu^{22} and $_{15}$Glu^8 are also exposed at the surface of the complex near the entrance of the channel, and Asp72 corresponds to one of the possible iron "anchors" $_{15}$His^{96}. In Nqo15, there is also glutamate 98 next to this histidine, closer to the entrance to the channel. Another anchor located deeper in the channel, $_{15}$His^{94}, is conserved between Nqo15 and bacterial frataxins.

Recently, the structure of the yeast frataxin trimer was determined with an Fe atom coordinated at the trimer interface by Asp143, corresponding to CyaY Asp72 and to $_{15}$His^{96} of complex I (*72*). It is likely that in vivo iron is carried by such multimers to protein partners. However, direct contact and iron delivery to the partner could involve only a monomer. The structure of frataxin bound to another protein is not yet available. Nqo15 appears to be a good model of such an interaction, as most residues implicated in iron binding for frataxins are very well positioned in complex I to deliver iron from the solvent to the putative sites at the

deep end of the channel. Also, frataxins are predicted to bind to the partners via the exposed face of the β-sheet (*73*), similar to Nqo15. To determine whether putative sites in complex I do bind iron, crystallization experiments in the presence of Fe(II) are underway.

Concluding Remarks

Although the structure of the hydrophilic domain answered many questions about complex I, it also has raised new ones. One of the most pressing issues is the role of cluster N1a and whether it is important mostly for the coupling between two- to one-electron carriers and thus reducing the level of ROS production. The current prediction is that if cluster N1a is removed, complex I would still be reasonably active but that the level of ROS production would increase. This hypothesis can be tested by mutating residues that coordinate, or interact with, N1a. Another crucial unanswered question is the nature of the coupling mechanism. Although the complete enzyme structure would be required to understand this mechanism, the structure of the hydrophilic domain reduced by NADH would also provide some clues. NADH-induced conformational changes, identified by proteolysis, cross-linking, and electron microscopy (*46*, *47*), may be present to their full extent only in the complete enzyme. In the case of the mitochondrial enzyme, the "activated" rather than "deactivated" enzyme (*74*) may be required. However, at least to some extent, these changes are likely to be present also in the isolated hydrophilic domain, and work to determine the structure in the presence of NADH is underway in my laboratory.

ACKNOWLEDGMENT

I thank Prof. John E. Walker for helpful discussions about the manuscript.

REFERENCES

1. Walker, J. E. (1992) The NADH-ubiquinone oxidoreductase (complex I) of respiratory chains, *Q. Rev. Biophys. 25*, 253−324.
2. Yagi, T., and Matsuno-Yagi, A. (2003) The proton-translocating NADH-quinone oxidoreductase in the respiratory chain: The secret unlocked, *Biochemistry 42*, 2266−2274.
3. Carroll, J., Fearnley, I. M., Shannon, R. J., Hirst, J., and Walker, J. E. (2003) Analysis of the subunit composition of complex I from bovine heart mitochondria, *Mol. Cell. Proteomics 2*, 117−126.
4. Carroll, J., Fearnley, I. M., Skehel, J. M., Shannon, R. J., Hirst, J., and Walker, J. E. (2006) Bovine complex I is a complex of 45 different subunits, *J. Biol. Chem. 281*, 32724−32727.
5. Hinchliffe, P., Carroll, J., and Sazanov, L. A. (2006) Identification of a novel subunit of respiratory complex I from *Thermus thermophilus*, *Biochemistry 45*, 4413−4420.
6. Grigorieff, N. (1998) Three-dimensional structure of bovine NADH:ubiquinone oxidoreductase (complex I) at 22 Å in ice, *J. Mol. Biol. 277*, 1033−1046.
7. Peng, G., Fritzsch, G., Zickermann, V., Schagger, H., Mentele, R., Lottspeich, F., Bostina, M., Radermacher, M., Huber, R., Stetter, K. O., and Michel, H. (2003) Isolation, characterization and electron microscopic single particle analysis of the NADH: ubiquinone oxidoreductase (complex I) from the hyperthermophilic eubacterium *Aquifex aeolicus*, *Biochemistry 42*, 3032−3039.
8. Guenebaut, V., Schlitt, A., Weiss, H., Leonard, K., and Friedrich, T. (1998) Consistent structure between bacterial and mitochondrial NADH:ubiquinone oxidoreductase (complex I), *J. Mol. Biol. 276*, 105−112.
9. Sazanov, L. A., Carroll, J., Holt, P., Toime, L., and Fearnley, I. M. (2003) A role for native lipids in the stabilization and two-dimensional crystallization of the *Escherichia coli* NADH-ubiquinone oxidoreductase (Complex I), *J. Biol. Chem. 278*, 19483−19491.
10. Schapira, A. H. (1998) Human complex I defects in neurodegenerative diseases, *Biochim. Biophys. Acta 1364*, 261−270.
11. Balaban, R. S., Nemoto, S., and Finkel, T. (2005) Mitochondria, oxidants, and aging, *Cell 120*, 483−495.
12. Dawson, T. M., and Dawson, V. L. (2003) Molecular pathways of neurodegeneration in Parkinson's disease, *Science 302*, 819−822.
13. Ohnishi, T. (1998) Iron-sulfur clusters/semiquinones in complex I, *Biochim. Biophys. Acta 1364*, 186−206.
14. Hinchliffe, P., and Sazanov, L. A. (2005) Organization of iron-sulfur clusters in respiratory complex I, *Science 309*, 771−774.
15. Sazanov, L. A., and Hinchliffe, P. (2006) Structure of the hydrophilic domain of respiratory complex I from *Thermus thermophilus*, *Science 311*, 1430−1436.
16. Guenebaut, V., Vincentelli, R., Mills, D., Weiss, H., and Leonard, K. R. (1997) Three-dimensional structure of NADH-dehydrogenase from *Neurospora crassa* by electron microscopy and conical tilt reconstruction, *J. Mol. Biol. 265*, 409−418.
17. Radermacher, M., Ruiz, T., Clason, T., Benjamin, S., Brandt, U., and Zickermann, V. (2006) The three-dimensional structure of complex I from *Yarrowia lipolytica*: A highly dynamic enzyme, *J. Struct. Biol. 154*, 269−279.
18. Friedrich, T., and Scheide, D. (2000) The respiratory complex I of bacteria, archaea and eukarya and its module common with membrane-bound multisubunit hydrogenases, *FEBS Lett. 479*, 1−5.
19. Vignais, P. M., Billoud, B., and Meyer, J. (2001) Classification and phylogeny of hydrogenases, *FEMS Microbiol. Rev. 25*, 455−501.
20. Brandt, U. (2006) Energy converting NADH:quinone oxidoreductase (complex I), *Annu. Rev. Biochem. 75*, 69−92.
21. Oh, J. I., and Bowien, B. (1998) Structural analysis of the fds operon encoding the NAD^+-linked formate dehydrogenase of *Ralstonia eutropha*, *J. Biol. Chem. 273*, 26349−26360.
22. Galkin, A. S., Grivennikova, V. G., and Vinogradov, A. D. (1999) $H^+/2e^-$ stoichiometry in NADH-quinone reductase reactions catalyzed by bovine heart submitochondrial particles, *FEBS Lett. 451*, 157−161.
23. Page, C. C., Moser, C. C., Chen, X., and Dutton, P. L. (1999) Natural engineering principles of electron tunnelling in biological oxidation-reduction, *Nature 402*, 47−52.
24. Bertero, M. G., Rothery, R. A., Palak, M., Hou, C., Lim, D., Blasco, F., Weiner, J. H., and Strynadka, N. C. (2003) Insights into the respiratory electron transfer pathway from the structure of nitrate reductase A, *Nat. Struct. Biol. 10*, 681−687.
25. Smith, M. A., Finel, M., Korolik, V., and Mendz, G. L. (2000) Characteristics of the aerobic respiratory chains of the microaerophiles *Campylobacter jejuni* and *Helicobacter pylori*, *Arch. Microbiol. 174*, 1−10.
26. Peters, J. W., Lanzilotta, W. N., Lemon, B. J., and Seefeldt, L. C. (1998) X-ray crystal structure of the Fe-only hydrogenase (CpI) from *Clostridium pasteurianum* to 1.8 angstrom resolution, *Science 282*, 1853−1858.
27. Deckert, G., Warren, P. V., Gaasterland, T., Young, W. G., Lenox, A. L., Graham, D. E., Overbeek, R., Snead, M. A., Keller, M., Aujay, M., Huber, R., Feldman, R. A., Short, J. M., Olsen, G. J., and Swanson, R. V. (1998) The complete genome of the hyperthermophilic bacterium *Aquifex aeolicus*, *Nature 392*, 353−358.
28. Krishnamoorthy, G., and Hinkle, P. C. (1988) Studies on the electron transfer pathway, topography of iron-sulfur centers, and site of coupling in NADH-Q oxidoreductase, *J. Biol. Chem. 263*, 17566−17575.
29. Kotlyar, A. B., Sled, V. D., Burbaev, D. S., Moroz, I. A., and Vinogradov, A. D. (1990) Coupling site I and the rotenone-sensitive ubisemiquinone in tightly coupled submitochondrial particles, *FEBS Lett. 264*, 17−20.
30. Moser, C. C., Farid, T. A., Chobot, S. E., and Dutton, P. L. (2006) Electron tunneling chains of mitochondria, *Biochim. Biophys. Acta 1757*, 1096−1109.
31. Yankovskaya, V., Horsefield, R., Tornroth, S., Luna-Chavez, C., Miyoshi, H., Leger, C., Byrne, B., Cecchini, G., and Iwata, S. (2003) Architecture of succinate dehydrogenase and reactive oxygen species generation, *Science 299*, 700−704.

32. Anderson, R. F., Hille, R., Shinde, S. S., and Cecchini, G. (2005) Electron transfer within complex II. Succinate:ubiquinone oxidoreductase of *Escherichia coli*, *J. Biol. Chem. 280*, 33331−33337.
33. Lambert, A. J., and Brand, M. D. (2004) Inhibitors of the quinone-binding site allow rapid superoxide production from mitochondrial NADH:ubiquinone oxidoreductase (complex I), *J. Biol. Chem. 279*, 39414−39420.
34. Kudin, A. P., Bimpong-Buta, N. Y., Vielhaber, S., Elger, C. E., and Kunz, W. S. (2004) Characterization of superoxide-producing sites in isolated brain mitochondria, *J. Biol. Chem. 279*, 4127−4135.
35. Grivennikova, V. G., and Vinogradov, A. D. (2006) Generation of superoxide by the mitochondrial Complex I, *Biochim. Biophys. Acta 1757*, 553−561.
36. Zharova, T. V., and Vinogradov, A. D. (1997) A competitive inhibition of the mitochondrial NADH-ubiquinone oxidoreductase (complex I) by ADP-ribose, *Biochim. Biophys. Acta 1320*, 256−264.
37. Vinogradov, A. D. (1998) Catalytic properties of the mitochondrial NADH-ubiquinone oxidoreductase (complex I) and the pseudo-reversible active/inactive enzyme transition, *Biochim. Biophys. Acta 1364*, 169−185.
38. Murataliev, M. B., and Feyereisen, R. (2000) Functional interactions in cytochrome P450BM3. Evidence that NADP(H) binding controls redox potentials of the flavin cofactors, *Biochemistry 39*, 12699−12707.
39. Kussmaul, L., and Hirst, J. (2006) The mechanism of superoxide production by NADH:ubiquinone oxidoreductase (complex I) from bovine heart mitochondria, *Proc. Natl. Acad. Sci. U.S.A. 103*, 7607−7612.
40. Kashani-Poor, N., Zwicker, K., Kerscher, S., and Brandt, U. (2001) A central functional role for the 49-kDa subunit within the catalytic core of mitochondrial complex I, *J. Biol. Chem. 276*, 24082−24087.
41. Flemming, D., Schlitt, A., Spehr, V., Bischof, T., and Friedrich, T. (2003) Iron-sulfur cluster N2 of the *Escherichia coli* NADH: ubiquinone oxidoreductase (complex I) is located on subunit NuoB, *J. Biol. Chem. 278*, 47602−47609.
42. Gurrath, M., and Friedrich, T. (2004) Adjacent cysteines are capable of ligating the same tetranuclear iron-sulfur cluster, *Proteins 56*, 556−563.
43. Zwicker, K., Galkin, A., Drose, S., Grgic, L., Kerscher, S., and Brandt, U. (2006) The Redox-Bohr group associated with iron-sulfur cluster N2 of complex I, *J. Biol. Chem. 281*, 23013−23017.
44. Matzanke, B. F., Anemuller, S., Schunemann, V., Trautwein, A. X., and Hantke, K. (2004) FhuF, part of a siderophore-reductase system, *Biochemistry 43*, 1386−1392.
45. Xia, Z., Dai, W., Zhang, Y., White, S. A., Boyd, G. D., and Mathews, F. S. (1996) Determination of the gene sequence and the three-dimensional structure at 2.4 angstroms resolution of methanol dehydrogenase from *Methylophilus* W3A1, *J. Mol. Biol. 259*, 480−501.
46. Mamedova, A. A., Holt, P. J., Carroll, J., and Sazanov, L. A. (2004) Substrate-induced conformational change in bacterial complex I, *J. Biol. Chem. 279*, 23830−23836.
47. Belogrudov, G., and Hatefi, Y. (1994) Catalytic sector of complex I (NADH:ubiquinone oxidoreductase): Subunit stoichiometry and substrate-induced conformation changes, *Biochemistry 33*, 4571−4576.
48. Hano, N., Nakashima, Y., Shinzawa-Itoh, K., and Yoshikawa, S. (2003) Effect of the side chain structure of coenzyme Q on the steady state kinetics of bovine heart NADH:coenzyme Q oxidoreductase, *J. Bioenerg. Biomembr. 35*, 257−265.
49. Holt, P. J., Morgan, D. J., and Sazanov, L. A. (2003) The location of NuoL and NuoM subunits in the membrane domain of the *Escherichia coli* complex I: Implications for the mechanism of proton pumping, *J. Biol. Chem. 278*, 43114−43120.
50. Sazanov, L. A., and Walker, J. E. (2000) Cryo-electron crystallography of two sub-complexes of bovine complex I reveals the relationship between the membrane and peripheral arms, *J. Mol. Biol. 302*, 455−464.
51. Baranova, E. A., Morgan, D. J., and Sazanov, L. A. (2006) Single particle analysis confirms distal location of subunits NuoL and NuoM in *E. coli* complex I, *J. Struct. Biol.* (in press).
52. Toyoshima, C., Nomura, H., and Tsuda, T. (2004) Lumenal gating mechanism revealed in calcium pump crystal structures with phosphate analogues, *Nature 432*, 361−368.
53. Moller, J. V., Olesen, C., Jensen, A. M., and Nissen, P. (2005) The structural basis for coupling of Ca^{2+} transport to ATP hydrolysis by the sarcoplasmic reticulum Ca^{2+}-ATPase, *J. Bioenerg. Biomembr. 37*, 359−364.
54. Rost, B., Yachdav, G., and Liu, J. (2004) The PredictProtein server, *Nucleic Acids Res. 32*, W321−W326.
55. Sazanov, L. A., Peak-Chew, S. Y., Fearnley, I. M., and Walker, J. E. (2000) Resolution of the membrane domain of bovine complex I into subcomplexes: Implications for the structural organization of the enzyme, *Biochemistry 39*, 7229−7235.
56. Friedrich, T. (2001) Complex I: A chimaera of a redox and conformation-driven proton pump? *J. Bioenerg. Biomembr. 33*, 169−177.
57. Chen, Y. R., Chen, C. L., Zhang, L., Green-Church, K. B., and Zweier, J. L. (2005) Superoxide generation from mitochondrial NADH dehydrogenase induces self-inactivation with specific protein radical formation, *J. Biol. Chem. 280*, 37339−37348.
58. Velazquez, I., Nakamaru-Ogiso, E., Yano, T., Ohnishi, T., and Yagi, T. (2005) Amino acid residues associated with cluster N3 in the NuoF subunit of the proton-translocating NADH-quinone oxidoreductase from *Escherichia coli*, *FEBS Lett. 579*, 3164−3168.
59. Yano, T., Sklar, J., Nakamaru-Ogiso, E., Takahashi, Y., Yagi, T., and Ohnishi, T. (2003) Characterization of cluster N5 as a fast-relaxing [4Fe-4S] cluster in the Nqo3 subunit of the proton-translocating NADH-ubiquinone oxidoreductase from *Paracoccus denitrificans*, *J. Biol. Chem. 278*, 15514−15522.
60. Waletko, A., Zwicker, K., Abdrakhmanova, A., Zickermann, V., Brandt, U., and Kerscher, S. (2005) Histidine 129 in the 75-kDa subunit of mitochondrial complex I from *Yarrowia lipolytica* is not a ligand for [Fe4S4] cluster N5 but is required for catalytic activity, *J. Biol. Chem. 280*, 5622−5625.
61. Djafarzadeh, R., Kerscher, S., Zwicker, K., Radermacher, M., Lindahl, M., Schagger, H., and Brandt, U. (2000) Biophysical and structural characterization of proton-translocating NADH-dehydrogenase (complex I) from the strictly aerobic yeast *Yarrowia lipolytica*, *Biochim. Biophys. Acta 1459*, 230−238.
62. Jormakka, M., Richardson, D., Byrne, B., and Iwata, S. (2004) Architecture of NarGH reveals a structural classification of MobisMGD enzymes, *Structure 12*, 95−104.
63. Grivennikova, V. G., Kapustin, A. N., and Vinogradov, A. D. (2001) Catalytic activity of NADH-ubiquinone oxidoreductase (complex I) in intact mitochondria. Evidence for the slow active/inactive transition, *J. Biol. Chem. 276*, 9038−9044.
64. Sharpley, M. S., and Hirst, J. (2006) The Inhibition of Mitochondrial Complex I (NADH:Ubiquinone Oxidoreductase) by Zn^{2+}, *J. Biol. Chem. 281*, 34803−34809.
65. Iuso, A., Scacco, S., Piccoli, C., Bellomo, F., Petruzzella, V., Trentadue, R., Minuto, M., Ripoli, M., Capitanio, N., Zeviani, M., and Papa, S. (2006) Dysfunctions of cellular oxidative metabolism in patients with mutations in the NDUFS1 and NDUFS4 genes of complex I, *J. Biol. Chem. 281*, 10374−10380.
66. Ricci, J. E., Munoz-Pinedo, C., Fitzgerald, P., Bailly-Maitre, B., Perkins, G. A., Yadava, N., Scheffler, I. E., Ellisman, M. H., and Green, D. R. (2004) Disruption of mitochondrial function during apoptosis is mediated by caspase cleavage of the p75 subunit of complex I of the electron transport chain, *Cell 117*, 773−786.
67. Flemming, D., Hellwig, P., and Friedrich, T. (2003) Involvement of tyrosines 114 and 139 of subunit NuoB in the proton pathway around cluster N2 in *Escherichia coli* NADH:ubiquinone oxidoreductase, *J. Biol. Chem. 278*, 3055−3062.
68. Hellwig, P., Scheide, D., Bungert, S., Mantele, W., and Friedrich, T. (2000) FT-IR spectroscopic characterization of NADH: ubiquinone oxidoreductase (complex I) from *Escherichia coli*: Oxidation of FeS cluster N2 is coupled with the protonation of an aspartate or glutamate side chain, *Biochemistry 39*, 10884−10891.
69. Huynen, M. A., Snel, B., Bork, P., and Gibson, T. J. (2001) The phylogenetic distribution of frataxin indicates a role in iron-sulfur cluster protein assembly, *Hum. Mol. Genet. 10*, 2463−2468.
70. Nair, M., Adinolfi, S., Pastore, C., Kelly, G., Temussi, P., and Pastore, A. (2004) Solution structure of the bacterial frataxin ortholog, CyaY: Mapping the iron binding sites, *Structure 12*, 2037−2048.
71. Costas, M., Mehn, M. P., Jensen, M. P., and Que, L., Jr. (2004) Dioxygen activation at mononuclear nonheme iron active sites: Enzymes, models, and intermediates, *Chem. Rev. 104*, 939−986.
72. Karlberg, T., Schagerlof, U., Gakh, O., Park, S., Ryde, U., Lindahl, M., Leath, K., Garman, E., Isaya, G., and Al-Karadaghi, S. (2006)

The structures of frataxin oligomers reveal the mechanism for the delivery and detoxification of iron, *Structure 14*, 1535−1546.
73. Cho, S. J., Lee, M. G., Yang, J. K., Lee, J. Y., Song, H. K., and Suh, S. W. (2000) Crystal structure of *Escherichia coli* CyaY protein reveals a previously unidentified fold for the evolutionarily conserved frataxin family, *Proc. Natl. Acad. Sci. U.S.A. 97*, 8932−8937.
74. Gostimskaya, I. S., Cecchini, G., and Vinogradov, A. D. (2006) Topography and chemical reactivity of the active-inactive transition-sensitive SH-group in the mitochondrial NADH:ubiquinone oxidoreductase (Complex I), *Biochim. Biophys. Acta 1757*, 1155−1161.
75. Grad, L. I., and Lemire, B. D. (2004) Mitochondrial complex I mutations in *Caenorhabditis elegans* produce cytochrome c oxidase deficiency, oxidative stress and vitamin-responsive lactic acidosis, *Hum. Mol. Genet. 13*, 303−314.
76. Grad, L. I., and Lemire, B. D. (2006) Riboflavin enhances the assembly of mitochondrial cytochrome c oxidase in *C. elegans* NADH-ubiquinone oxidoreductase mutants, *Biochim. Biophys. Acta 1757*, 115−122.
77. Duarte, M., Schulte, U., Ushakova, A. V., and Videira, A. (2005) *Neurospora* strains harboring mitochondrial disease-associated mutations in iron-sulfur subunits of complex I, *Genetics 171*, 91−99.
78. Benit, P., Chretien, D., Kadhom, N., de Lonlay-Debeney, P., Cormier-Daire, V., Cabral, A., Peudenier, S., Rustin, P., Munnich, A., and Rotig, A. (2001) Large-scale deletion and point mutations of the nuclear NDUFV1 and NDUFS1 genes in mitochondrial complex I deficiency, *Am. J. Hum. Genet. 68*, 1344−1352.
79. Kerscher, S., Benit, P., Abdrakhmanova, A., Zwicker, K., Rais, I., Karas, M., Rustin, P., and Brandt, U. (2004) Processing of the 24 kDa subunit mitochondrial import signal is not required for assembly of functional complex I in *Yarrowia lipolytica*, *Eur. J. Biochem. 271*, 3588−3595.
80. Martin, M. A., Blazquez, A., Gutierrez-Solana, L. G., Fernandez-Moreira, D., Briones, P., Andreu, A. L., Garesse, R., Campos, Y., and Arenas, J. (2005) Leigh syndrome associated with mitochondrial complex I deficiency due to a novel mutation in the NDUFS1 gene, *Arch. Neurol. 62*, 659−661.
81. Kerscher, S., Grgic, L., Garofano, A., and Brandt, U. (2004) Application of the yeast *Yarrowia lipolytica* as a model to analyse human pathogenic mutations in mitochondrial complex I (NADH: ubiquinone oxidoreductase), *Biochim. Biophys. Acta 1659*, 197−205.
82. Grgic, L., Zwicker, K., Kashani-Poor, N., Kerscher, S., and Brandt, U. (2004) Functional significance of conserved histidines and arginines in the 49-kDa subunit of mitochondrial complex I, *J. Biol. Chem. 279*, 21193−21199.
83. Prieur, I., Lunardi, J., and Dupuis, A. (2001) Evidence for a quinone binding site close to the interface between NUOD and NUOB subunits of Complex I, *Biochim. Biophys. Acta 1504*, 173−178.
84. Ahlers, P. M., Zwicker, K., Kerscher, S., and Brandt, U. (2000) Function of conserved acidic residues in the PSST homologue of complex I (NADH:ubiquinone oxidoreductase) from *Yarrowia lipolytica*, *J. Biol. Chem. 275*, 23577−23582.
85. Garofano, A., Zwicker, K., Kerscher, S., Okun, P., and Brandt, U. (2003) Two aspartic acid residues in the PSST-homologous NUKM subunit of complex I from *Yarrowia lipolytica* are essential for catalytic activity, *J. Biol. Chem. 278*, 42435−42440.
86. Ahlers, P. M., Garofano, A., Kerscher, S. J., and Brandt, U. (2000) Application of the obligate aerobic yeast *Yarrowia lipolytica* as a eucaryotic model to analyse Leigh syndrome mutations in the complex I core subunits PSST and TYKY, *Biochim. Biophys. Acta 1459*, 258−265.
87. Flemming, D., Hellwig, P., Lepper, S., Kloer, D. P., and Friedrich, T. (2006) Catalytic importance of acidic amino acids on subunit NuoB of the *Escherichia coli* NADH:ubiquinone oxidoreductase (complex I), *J. Biol. Chem. 281*, 24781−24789.
88. Chevallet, M., Dupuis, A., Issartel, J. P., Lunardi, J., van Belzen, R., and Albracht, S. P. (2003) Two EPR-detectable [4Fe-4S] clusters, N2a and N2b, are bound to the NuoI (TYKY) subunit of NADH:ubiquinone oxidoreductase (Complex I) from *Rhodobacter capsulatus*, *Biochim. Biophys. Acta 1557*, 51−66.

BI602508X